

Robust Optimal Safe and Stability Guaranteeing Reinforcement Learning Control for Quadcopter

Sanghyoup Gu, *Student Member, IEEE*; Ratnesh Kumar, *Fellow, IEEE*

Abstract—Recent advances in deep learning has provided new data-driven ways of controller design, to replace the traditional manual synthesis and certification approaches. Employing neural network (NN) as controllers however presents its own challenge: that of certifying stability, due to their inherent complex nonlinearity, and while NN controllers have demonstrated high performance in complex systems, they often lack formal stability guarantees. This issue is further accentuated for critical nonlinear applications such as of unmanned aerial vehicles (UAVs), complicating their stability guarantees, whereas a lack of stability assurance raises the risk of critical damage or even complete failure under a loss of control. In this study, we improve a Robust, Optimal, Safe and Stability Guaranteed Training (ROSS-GT) method of [1] to design an NN controller for a quadcopter flight control. The approach ensures closed-loop system stability by finding a Lyapunov function, and providing a safe initial state domain that remains invariant under the control and guarantees stability to an equilibrium within it. Stability guaranteeing constraints are derived from the sector bound of the system nonlinearity and of its parameters and disturbance variations, in the form of a Lipschitz bound for a NN control. The control performance is further optimized by searching over the class of stability-guaranteeing controllers to minimize the reference tracking error and the control costs.

Index Terms—Neural Network Controller, Robust Control, Stability Guarantee, Reinforcement Learning

I. INTRODUCTION

IN recent decades, neural networks (NNs) based data-driven approach has achieved great progress, finding applications across diverse fields. One promising usecase is in the design of NN controllers for dynamical systems, where a neural network maps states or observations to actions. Unlike conventional feedback controllers, which rely either on predefined structures with domain-specific expertise for their tuning or control Lyapunov functions requiring manual exploration, NN controllers are trained through data-driven approaches. For instance, supervised imitation learning uses images from a human operator and trains a neural network to imitate those actions [2], [3]. Similarly, in reinforcement learning (RL), policy networks are optimized to maximize the expected cumulative rewards from control sequences [4].

While NN controllers have demonstrated good performance in many applications, their deployment in safety-critical systems, such as unmanned aerial vehicles (UAVs), remains limited due to the lack of formal stability guarantees. Yet

another important consideration for controllers is robustness—the ability of a system to withstand disturbances, sensor noise, or model uncertainties without loss of stability. In real-world environments characterized by various uncertainties, robust control is essential to ensure reliable operation, which again requires a formal certification that in general is lacking for NN controllers.

This paper enhances and applies the Robust, Optimal, Safe and Stability-Guaranteed Training (ROSS-GT) method of [1] to design and train an NN controller for a quadcopter, a widely used form of UAV. The ROSS-GT method consists of two stages: First, it extracts the constraints to ensure robust stability and safety for a closed-loop system as well as a safe initial state domain that is invariant and guarantees converges to an equilibrium within, based on the sector bounds of system nonlinearities and bounds for parametric variations and disturbances, in form of a Lipschitz bound for the neural network (i.e., their output needs to be bounded by the input magnitude and the Lipschitz bound gain). The maximal permissible robust, safe, and stabilizing Lipschitz bound and the initial safe state domain ensuring asymptotic stability under bounded parametric uncertainty and disturbance are derived by iteratively solving a linear matrix inequality (LMI) test. Second, it finds an optimal NN controller satisfying the Lipschitz bound obtained in the first step to minimize control cost and reference trajectory deviation error using reinforcement learning.

The original ROSS-GT method [1] employs the infinity norm to derive the Lipschitz bound for the NN controller. However, this approach often yields overly conservative estimates for the NN Lipschitz constant, particularly for NN with many neurons, making it impractical. In this paper, we propose an enhancement, replacing the infinity norm with the Euclidean norm, demonstrating that it still satisfies the LMI constraints, while reducing the above mentioned conservativeness. Furthermore, we utilize a semidefinite programming-based method for the estimation of Lipschitz constant of a neural network [5] that again enhances the method in [1], enabling less conservative bounds and enhancing the practicality of robust, safety-and-stability-guaranteeing NN controller design.

A. Related Work on learning-based control

In imitation learning setting of [2], a human expert remotely controls a drone equipped with a camera to follow a moving object on the ground. The video recording of the human expert collected during this process is subsequently used to train a neural network to imitate the expert's command for

the corresponding raw inputs. In the reinforcement learning (RL) setting of [6], a deterministic on-policy gradient method was applied to train a NN controller for a quadcopter to recover its position under harsh disturbances, demonstrating its stabilizing ability, but without any formal guarantee. Studies in [7], comparing deep RL methods such as Deep Deterministic Policy Gradient (DDPG), Trust Region Policy Optimization (TRPO), and Proximal Policy Optimization (PPO) with traditional PID controllers found that RL-trained NN controllers outperformed their PID counterparts in attitude control tasks. These findings highlight the potential of NN controllers for quadcopter control, often achieving performances better than the conventional methods.

However, a critical limitation of these approaches is their lack of formal guarantee of stability and robustness to environmental and model uncertainties. Such limitation hinder the transferability of NN controllers trained in one environment to another. To address this, researchers have explored methods to robustify the training of NN controllers. Domain randomization, for example, has been employed to account for uncertainties by randomizing model/disturbance parameters during the training. This method enabled a quadcopter to land autonomously at a target point [8], with results showing that the adequately randomized domains allowed the trained policy to generalize to new environments without any additional training. Similarly, the Robust Markov Decision Process (RMDP) was used in [9] to handle environmental and model uncertainties, where RMDP maximizes cumulative rewards under worst-case scenarios. Quadcopter attitude control trained using RMDP demonstrated satisfactory trajectory tracking in uncertain environments [9]. While these methods improve robustness, they lack any formal guarantee.

From a control theory perspective, some studies have analyzed NN controllers to ensure stability. For instance, [10] introduced a quadratic constraint for Lipschitz functions, formulating a semidefinite programming problem to guarantee input-output stability. [1] developed quadratic constraint for Lipschitz-bounded NN controllers, sector bounded nonlinear components of the system and bound for its variability and disturbances, deriving linear matrix inequality (LMI) constraints for robust Lyapunov stability.

To the best of our knowledge, our work is the first that leverages these advancements of robust, safe, and stability-guaranteed NN control design for the navigation of quadcopters for optimal reference trajectory tracking. Our contribution further includes enhancing the method of [1] to allow for less conservative Lipschitz bound by using 2-norm in place of infinity-norm while preserving the key results of robust stability, and by estimating the Lipschitz bound of a NN controller using a less conservative method involving semi-definite programming.

B. Organization

The remainder of this paper is organized as follows. Section II briefly discusses quadcopter dynamics. Section III reviews the robust optimal safe and stability-guaranteed training (ROSS-GT) method of [1]. Section IV presents the

enhancement and application of ROSS-GT for a quadcopter. Section V provides the simulation results of the trained NN controller. Section VI then provides a conclusion.

C. Notation

For a vector $x \in \mathbb{R}^n$, x_i denotes its i -th element. $\|x\|_p$ denotes vector's p norm when $p \geq 1$ and $\|x\|_\infty$ denotes the infinity norm, $diag(x)$ denotes a diagonal matrix whose i -th diagonal element is x_i . For a matrix $M \in \mathbb{R}^{m \times n}$, M_{ij} denotes its element in i -th row and j -th column. A symmetric matrix is denoted by $P = \begin{bmatrix} P_{11} & * \\ P_{21} & P_{22} \end{bmatrix}$. \mathbb{S} , $\mathbb{S}^{\geq 0}$, and \mathbb{S}^+ represent the set of symmetric, positive semi-definite, and positive definite matrices, respectively.

II. QUADCOPTER MODEL

In this section, quadcopter dynamics is briefly discussed. Quadcopter dynamics consists of translation and rotation movement. In the case of translation movement, gravitation and thrust contribute to the acceleration. Also, the drag force, which is proportional to the velocity, also impacts the translation motion.

$$m \begin{bmatrix} \ddot{x} \\ \ddot{y} \\ \ddot{z} \end{bmatrix} = \begin{bmatrix} 0 \\ 0 \\ -g \end{bmatrix} + \mathbf{R} \begin{bmatrix} 0 \\ 0 \\ T \end{bmatrix} - \mathbf{D} \begin{bmatrix} \dot{x} \\ \dot{y} \\ \dot{z} \end{bmatrix}, \quad (1)$$

where $[x, y, z]^T \in \mathbb{R}^3$ is the position in the inertial frame, m is the mass, g is the gravitational acceleration, T is the thrust produced from the propellers, $\mathbf{R} \in SO(3)$ is the rotation matrix from the body frame to the inertial frame [$SO(3)$ is special orthogonal group, i.e., $SO(3) = \{\mathbf{R} \in \mathbb{R}^3 | \mathbf{R}^T \mathbf{R} = I, \det(\mathbf{R}) = 1\}$], and $\mathbf{D} = diag([D_x, D_y, D_z]^T)$ is the diagonal drag coefficient matrix. The rotation matrix \mathbf{R} is given by the equality (2) involving the Euler angles $[\phi, \theta, \psi] \in \mathbb{R}^3$ of roll, pitch, and yaw between the inertial and the body frames:

$$\mathbf{R} = \begin{bmatrix} C_\psi C_\theta & C_\psi S_\theta S_\phi - S_\psi C_\phi & C_\psi S_\theta C_\phi + S_\psi S_\phi \\ S_\psi C_\theta & S_\psi S_\theta S_\phi + C_\psi C_\phi & S_\psi S_\theta C_\phi - C_\psi S_\phi \\ -S_\theta & C_\theta S_\phi & C_\theta C_\phi \end{bmatrix}, \quad (2)$$

where S_a and C_a indicates $\sin(a)$ and $\cos(a)$, respectively.

In the case of rotation movement, the angular acceleration in the body frame is produced by the centripetal force and the torque. The gyroscopic force is neglected because it is much smaller than the other two components.

$$\begin{bmatrix} \dot{p} \\ \dot{q} \\ \dot{r} \end{bmatrix} = \begin{bmatrix} (I_{yy} - I_{zz})qr/I_{xx} \\ (I_{zz} - I_{xx})pr/I_{yy} \\ (I_{xx} - I_{yy})pq/I_{zz} \end{bmatrix} + \begin{bmatrix} \tau_\phi/I_{xx} \\ \tau_\theta/I_{yy} \\ \tau_\psi/I_{zz} \end{bmatrix}, \quad (3)$$

where $[p, q, r]^T \in \mathbb{R}^3$ is the angular velocity in the body frame, $[I_{xx}, I_{yy}, I_{zz}]$ are the three moment of inertia components, and $[\tau_\phi, \tau_\theta, \tau_\psi]^T$ is the torque produced from the propellers.

In this work, an X-shape quadcopter is considered. Thus, the thrust and torque values are generated by the individual propeller's rotations and thrust and drag constants:

$$\begin{bmatrix} T \\ \tau_\phi \\ \tau_\theta \\ \tau_\psi \end{bmatrix} = \begin{bmatrix} k_t & k_t & k_t & k_t \\ -\frac{lk_t}{\sqrt{2}} & -\frac{lk_t}{\sqrt{2}} & \frac{lk_t}{\sqrt{2}} & \frac{lk_t}{\sqrt{2}} \\ -\frac{lk_t}{\sqrt{2}} & \frac{lk_t}{\sqrt{2}} & \frac{lk_t}{\sqrt{2}} & -\frac{lk_t}{\sqrt{2}} \\ k_d & -k_d & k_d & -k_d \end{bmatrix} \begin{bmatrix} \omega_1^2 \\ \omega_2^2 \\ \omega_3^2 \\ \omega_4^2 \end{bmatrix}, \quad (4)$$

where ω_i is the angular speed of the i th rotor, l is the length of each arm of the quadcopter, k_t is the thrust constant, and k_d is the drag constant. A more detailed explanation for quadcopter dynamics modeling can be found in [11].

III. ROBUST OPTIMAL SAFE AND STABILITY GUARANTEED TRAINING METHOD

We apply the Robust Optimal Safe and Stability Guaranteed Training (ROSS-GT) method proposed in [1] to certify the safety and asymptotic stability of neural network (NN)-controlled closed-loop systems with parameter variations and environmental disturbances. Robust asymptotic stability is guaranteed by finding a robust Lyapunov function for the system, which provides a sufficient condition for stability, and a neighborhood of the equilibrium that is a sublevel set of the Lyapunov function serves as a safe invariant domain for initialization.

A. System and Control Framework

The system under consideration consists of nonlinear dynamics with parameter variations, representing model uncertainties or disturbances:

$$\begin{aligned} \dot{s}(t) &= f(s(t), u(t), \alpha(t)), \\ u(t) &= \pi(s(t)) = \pi_0(s(t)) + \pi_{NN}(s(t)) \end{aligned} \quad (5)$$

where $s(t) \in \mathbb{R}^n$, $u(t) \in \mathbb{R}^m$, and $\alpha(t) \in \mathbb{R}^d$ are state, control input, and parameter variation, respectively; $f: \mathbb{R}^n \times \mathbb{R}^m \times \mathbb{R}^d \rightarrow \mathbb{R}^n$ denotes the nonlinear plant dynamics assumed to be locally continuously differentiable; $\pi: \mathbb{R}^n \rightarrow \mathbb{R}^m$ denotes a state-feedback control policy that is viewed as composition of nominal $\pi_0(\cdot)$ and NN $\pi_{NN}(\cdot)$ controllers.

An equilibrium point is defined as the state where the system dynamics remains unchanged ($\dot{s} = 0$). The equilibrium point is assumed invariant under parameter variations, and without loss of generality, the coordinates are shifted such that the equilibrium point aligns with the origin ($s^* = 0$). The system (5) is deemed robustly asymptotically stable if, starting from an initial state within a certain neighborhood of the equilibrium, it converges to the equilibrium point in spite of the parametric variations, assumed to be bounded within a hyper-rectangular, providing upper and lower bounds for the parameters.

When parameter variations are zero, the system is referred to as the nominal system, and the corresponding control is termed the nominal control, and is designed to stabilize the nominal system linearized around the equilibrium point. The NN control is thus viewed as a perturbation around the nominal control

to ensure the stability of the overall parameter-varying system (and not just the linearized nominal system). Fig 1 illustrates the structure of the control architecture, which integrates both the nominal and NN controllers. Both the nominal and NN controllers operate as state-feedback controllers, with the plant receiving control commands as the sum of their respective outputs.

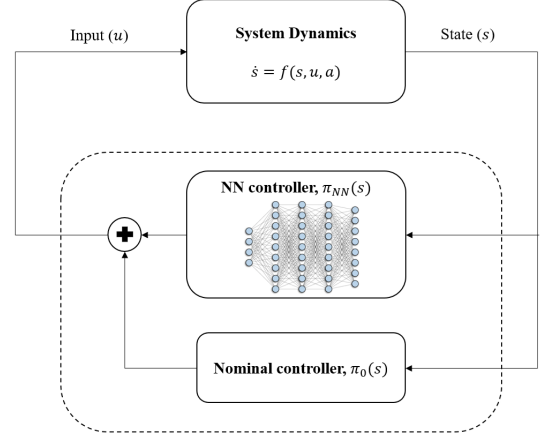


Fig. 1: Control Architecture

Definition 1 (Lyapunov function [12]) For a dynamical system with an equilibrium point s^* , a continuously differentiable function $\mathcal{V}: \mathcal{S} \rightarrow \mathbb{R}_{\geq 0}$, where $\mathcal{S} \subset \mathbb{R}^n$ is a compact domain such that $s^* \in \mathbf{int}(\mathcal{S})$, is a Lyapunov function and \mathcal{S} is region-of-stability (RoS) if:

$$\begin{aligned} \mathcal{V}(s) &> 0, \dot{\mathcal{V}}(s) < 0, \forall s \in \mathcal{S} \setminus s^*; \\ \mathcal{V}(s^*) &= \dot{\mathcal{V}}(s^*) = 0, \end{aligned}$$

where $\mathbf{int}(\mathcal{S})$ denotes the interior of \mathcal{S} .

In [1], a feasibility condition for the existence of a Lyapunov function comes from two quadratic constraints (QC) obtained from: 1) NN controller Lipschitz bound, and 2) nonlinear and parameter variation (NPV) sector bound. As demonstrated in [10], Lipschitz continuous functions, such as the NNs, exhibit QCs derived from their bounded partial derivatives within a specified domain. Similarly, sector bounded NPVs imply another set of QCs. By combining these QCs, [1] proposed a Linear Matrix Inequality (LMI) constraint to be able to certify the existence of a Lyapunov function (the details are given below in this section itself).

The ROSS-GT method of [1] is implemented in two stages:

1. Extraction of maximal Lipschitz bound and robust and safe region of stability (RS-RoS):

From the given system dynamics with bounds for parameter variations and a safety domain, the maximal RS-RoS, the maximal Lipschitz bound for the NN controller, and a state-feedback gain of nominal controller are derived, iteratively, based on the feasibility of the LMI constraint.

2. Optimal NN Controller Training: A NN controller is then trained using reinforcement learning while ensuring that

its Lipschitz constant remains within the bound established in the first stage, and the cost of control and deviation from reference trajectory is minimized.

The original approach in [1] used the infinity norm for defining Lipschitz continuity and deriving QCs associated with the NN control. In this context, the Lipschitz constant of the NN controller was estimated using the maximum absolute row sum norm of its weight matrices. However, this approach often yields overly conservative estimates, particularly for high-dimensional networks, making it impractical. To address this, and make the approach of [1] practical, here we propose replacing the infinity norm with the Euclidean (L2) norm, proving that the feasibility of the LMI constraint is preserved under this change. Additionally, we employ a semidefinite programming-based method [5] to obtain tighter Lipschitz estimates, resulting in more practical relaxed Lipschitz bounds for the NN controllers.

B. Lipschitz Continuity of NN Controller and its QC

A neural network (NN) is a Lipschitz operator, meaning its output magnitude is bounded by the product of the Lipschitz constant and the input magnitude. The Lipschitz continuity of an NN can be defined using any type of norm; in this work, we adopt the L2-norm for the Lipschitz continuity.

Definition 2 (Lipschitz continuity) A function π is locally Lipschitz continuous over a domain \mathcal{S} if there exists a constant $L > 0$ such that:

$$\|\pi(x) - \pi(y)\|_2 \leq L \|x - y\|_2, \forall x, y \in \mathcal{S}. \quad (6)$$

where L is the Lipschitz bound constant. The class of all control maps $\pi(\cdot)$ that are L -Lipschitz is denoted by Π_L .

Neural networks are composed of linear operations and nonlinear activation functions. The linear operations have bounded gradients, with their Lipschitz constant determined by the largest singular value of the weight matrix. On the other hand, the nonlinear activation functions such as, Sigmoid, ReLU, and tanh, have Lipschitz constants between 0 and 1 [13]. Computing the exact Lipschitz constant of an NN is challenging due to the piecewise application of activation functions, making the gradient calculation complex. However, efficient estimation of the Lipschitz constant for NNs can be achieved using semidefinite programming (SDP) solvers [5].

As shown in [1, Proposition 1], each output of an NN can be expressed as a linear combination of scalar functions and input elements, with partial derivatives bounded between $-L$ and L . As shown next, this result remains valid even when using the L2-norm, ensuring that the Lipschitz continuity of the NN remains appropriately represented in the analysis. From the definition of Lipschitz continuity (6) and triangular inequality,

the NN controller π_{NN} satisfies the following:

$$\begin{aligned} \|\pi_{NN}(s_1) - \pi_{NN}(s_2)\|_2 &\leq L \|s_1 - s_2\|_2 \\ &= L \sqrt{\sum_{j=1}^n |s_{1,j} - s_{2,j}|^2} \\ &\leq L \sum_{j=1}^n |s_{1,j} - s_{2,j}|, \forall s_1, s_2 \in \mathbb{R}^n \end{aligned}$$

Also, the infinity-norm is always less than the 2-norm:

$$\|\pi_{NN}(s_1) - \pi_{NN}(s_2)\|_\infty \leq \|\pi_{NN}(s_1) - \pi_{NN}(s_2)\|_2.$$

From above two inequalities, the same result with [1, Proposition 1] is obtained even when we use 2-norm to define Lipschitz continuity (as opposed to the ∞ -norm):

$$\|\pi_{NN}(s_1) - \pi_{NN}(s_2)\|_\infty \leq L \sum_{j=1}^n |s_{1,j} - s_{2,j}|.$$

It then follows that there exists a set of scalar functions: $\delta_{ij} : \mathbb{R}^n \times \mathbb{R}^n \rightarrow [-L, L], \forall i \in \{1, \dots, m\}, \forall j \in \{1, \dots, n\}$ such that $\forall s_1, s_2 \in \mathbb{R}^n$:

$$\pi_{NN}(s_1) - \pi_{NN}(s_2) = \begin{bmatrix} \sum_{j=1}^n \delta_{1j}(s_1, s_2)(s_{1,j} - s_{2,j}) \\ \vdots \\ \sum_{j=1}^n \delta_{mj}(s_1, s_2)(s_{1,j} - s_{2,j}) \end{bmatrix},$$

which is the same core result in the proof of [1, Proposition 1]. Therefore, the QC of [1, Proposition 1] is still valid even under the use of L2-norm based Lipschitz continuity. Note the change in norm, results in a new version of the input domain implied by the state domain \mathcal{S} :

$$\begin{aligned} \mathcal{U}_{L,\mathcal{S}} := \{u_{NN} \in \mathbb{R}^m \mid \exists s \in \mathcal{S}, \pi_{NN}(s) = u_{NN}, \\ \|u_{NN}\|_2 \leq L \|s\|_2\}. \quad (7) \end{aligned}$$

C. Sector bound of nonlinear and parameter variation and its QC

The system of (5) under nominal state-feedback control $\pi_0(s) = Ks$ can be decomposed into linear and ‘‘nonlinear and parameter variation (NPV)’’ components, by linearization of the nominal system around the equilibrium and considering the rest of the nonlinearity:

$$\dot{s}(t) = \underbrace{(A_0 + B_0K)}_{A_K} s(t) + \underbrace{B_0u_{NN}(t) + \eta(s(t), u_{NN}(t), \alpha(t))}_{\text{NPV: } \eta(s(t), u_{NN}(t), \alpha(t))}$$

where $u_{NN}(t) = \pi_{NN}(s(t))$, the entries in the linearized nominal part are obtained from the Jacobians of f and π (that exist owing to their local continuous differentiability assumption) as follows:

$$A_K := (J_{f,s} + J_{f,u}J_{\pi,s})|_{s=0, u_{NN}=0, \alpha=0} = A_0 + B_0K,$$

and $\eta(s, u_{NN}, \alpha) = f(s, Ks + u_{NN}, \alpha) - A_Ks - B_0u_{NN}$ is the remaining additive nonlinear part. The overall NPV part is the component not included in the linearized nominal part, namely:

$$\zeta(s(t), u_{NN}(t), \alpha(t)) = B_0u_{NN}(t) + \eta(s(t), u_{NN}(t), \alpha(t)).$$

The sector bounds of the NPV component over the state and input domains $\mathcal{S}, \mathcal{U}_{L,S}$, respectively, are then derived as the bounds for the Jacobians of the NPV, ζ :

$$\begin{aligned} \underline{\mathcal{L}}^{i,j} &\leq J_{\zeta,s}^{i,j} \leq \bar{\mathcal{L}}^{i,j}, \forall i, j \in \{1, \dots, n\} \\ \underline{\mathcal{L}}^{i,j+n} &\leq J_{\zeta,u}^{i,j} \leq \bar{\mathcal{L}}^{i,j+n}, \forall i \in \{1, \dots, n\}, \forall j \in \{1, \dots, m\}. \end{aligned}$$

These sector bounds then imply the existence of another QC as formulated in [1, Proposition 2].

D. LMI for robust stability

Using the QCs for the NN controller Lipschitz bound and system NPV sector bound, in [1], an LMI constraint is obtained to guarantee the existence of a robust Lyapunov function over a given state domain, Lipschitz constant, and parameter variation bound. The feasibility of this LMI constraint ensures the existence of a robust quadratic Lyapunov function to certify the the stability of the NN-controlled system and a RoS within the specified safety set that is invariant and ensures convergence to equilibrium, even under parameter variations.

Theorem 1 (Linear Matrix Inequality Constraint [1])

For the given system of (5), when the below LMI constraint of (8) is feasible for some $L, K, (P > 0), (\Lambda \geq 0), (\gamma_{ij} \geq 0, \forall i \in 1, \dots, m, j \in 1, \dots, n)$ over the given state parameter variation domains, then there exists a robust quadratic Lyapunov function $\mathcal{V}(s) = s^T P s$ such that $\pi(s) = Ks + \pi_{NN}(s); \pi_{NN} \in \Pi_L$ stabilizes the system of (5) over the given state domain under the variations of the parameters in its given domain.

$$\begin{bmatrix} V_{L, \{\Gamma_j\}, P} & * & * \\ \mathbf{0}_{m,n \times n} & M_{\chi\Lambda} - \text{diag}(\{\gamma_{ij}\}) & * \\ N_{s\Lambda}^T + R^T \cdot P & N_{\chi\Lambda}^T & M_{\xi\Lambda} \end{bmatrix} \prec 0, \quad (8)$$

where $\Gamma_j := \sum_{i=1}^m \gamma_{ij}$ for all $j \in \{1, \dots, n\}$, and the matrices are defined as follows:

$$\begin{aligned} V_{L, \{\Gamma_j\}, P} &= M_{s\Lambda} + L^2 \cdot \text{diag}(\{\Gamma_j\}) + P A_K + A_K^T P; \\ M_{s\Lambda} &:= \text{diag} \left(\sum_{i=1}^n \Lambda^{k_{ij}} (\bar{c}_{ij}^2 - c_{ij}^2) \mid j \in 1, \dots, n \right); \\ k_{ij} &:= i + (j - 1)n; \\ c_{ij} &:= (\underline{\mathcal{L}}^{i,j} + \bar{\mathcal{L}}^{i,j})/2; \quad \bar{c}_{ij} := \max(|\underline{\mathcal{L}}^{i,j}|, |\bar{\mathcal{L}}^{i,j}|); \\ M_{\chi\Lambda} &:= Q^T \text{diag} \left(\sum_{i=1}^n \Lambda^{k_{ij}} (\bar{c}_{ij}^2 - c_{ij}^2) \mid j \in n + 1, \dots, n + m \right) Q; \\ Q &:= \mathbf{I}_m \odot \mathbf{1}_{1 \times n}; \quad R := \mathbf{I}_n \odot \mathbf{1}_{1 \times (n+m)}; \\ M_{\xi\Lambda} &:= \text{diag}(-\Lambda); \\ N_{s\Lambda} &:= [D_{s,1}, \dots, D_{s,n}]; \\ D_{s,i} &:= [\text{diag}(\Lambda^{k_{ij}} \cdot c_{ij} \mid j \in 1, \dots, n) \quad \mathbf{0}_{n \times m}]; \\ N_{\chi\Lambda} &:= Q^T \cdot [D_{\chi,1}, \dots, D_{\chi,n}]; \\ D_{\Lambda,i} &:= [\mathbf{0}_{m \times n} \text{diag}(\Lambda^{k_{ij}} \cdot c_{ij} \mid j \in n + 1, \dots, n + m)]. \end{aligned} \quad (9)$$

IV. ROBUST STABILIZING CONTROL FOR QUADCOPTER

A. Dynamics with parameter variation & Nominal control

We consider the Iris quadcopter [14] for control design, where Table I lists its parameter values.

TABLE I: Constant for Quadcopter Model

Parameter	Description	Value
I_{xx}, I_{yy}	x/y-axis rotational moment of inertia	$2.9125 \times 10^{-2} [kg \cdot m^2]$
I_{zz}	z-axis rotational moment of inertia	$5.5225 \times 10^{-2} [kg \cdot m^2]$
g	gravitational acceleration	$9.807 [m/s^2]$
m	mass	$1.5 [kg]$
l	distance between center and rotor	$0.25554 [m]$
k_d/k_t	ratio between drag and lift constants	0.06
D_x, D_y, D_z	x/y/z-axis drag coefficient	0.25

A quadcopter is an underactuated system where the degree of freedom for control is less than the number of states. Given a desired position (x_d, y_d, z_d) and heading (ψ_d) , a cascade proportional-derivative (PD) controller is employed as the nominal controller in our design. The positional P-controller computes the desired thrust (T_d) and roll/pitch angles (ϕ_d, θ_d) , which are then used by the attitude PD-controller to calculate the desired torque (τ_d) . The structure of this nominal controller is shown in Fig 2.

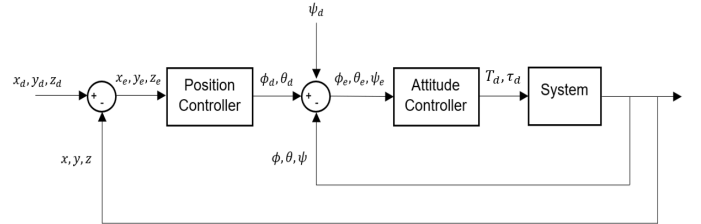


Fig. 2: Nominal Controller

The control inputs are set as the motor thrusts, which serve as the actuator commands to stabilize and guide the quadcopter:

$$u_i = k_t \omega_i^2, \forall i \in \{1, 2, 3, 4\},$$

and these control inputs are allocated from the required thrust and torques using:

$$\begin{bmatrix} u_1 \\ u_2 \\ u_3 \\ u_4 \end{bmatrix} = \begin{bmatrix} 1 & 1 & 1 & 1 \\ -\frac{l}{\sqrt{2}} & -\frac{l}{\sqrt{2}} & \frac{l}{\sqrt{2}} & \frac{l}{\sqrt{2}} \\ -\frac{l}{\sqrt{2}} & \frac{l}{\sqrt{2}} & \frac{l}{\sqrt{2}} & -\frac{l}{\sqrt{2}} \\ k_d/k_t & -k_d/k_t & k_d/k_t & -k_d/k_t \end{bmatrix}^{-1} \begin{bmatrix} T_d \\ \tau_{\phi,d} \\ \tau_{\theta,d} \\ \tau_{\psi,d} \end{bmatrix}.$$

Position Controller:

$$\begin{aligned} x_e &= x_d - x, y_e = y_d - y, z_e = z_d - z; \\ \phi_d &= -K_y y_e, \theta_d = K_x x_e, T_d = K_z z_e. \end{aligned}$$

Attitude Controller:

$$\begin{aligned}
\phi_e &= \phi_d - \phi = -K_y y_e - \dot{\phi}; \\
\theta_e &= \theta_d - \theta = K_x x_e - \dot{\theta}; \\
\psi_e &= \psi_d - \psi; \\
\tau_{\phi,d} &= K_\phi \dot{\phi}_e + K_{\dot{\phi}} \dot{\phi}_e; \\
&= K_\phi [-K_y (y_d - y) - \dot{\phi}] + K_{\dot{\phi}} [K_y \dot{y} - \dot{\phi}]; \\
\tau_{\theta,d} &= K_\theta \dot{\theta}_e + K_{\dot{\theta}} \dot{\theta}_e; \\
&= K_\theta [K_x (x_d - x) - \dot{\theta}] + K_{\dot{\theta}} [-K_x \dot{x} - \dot{\theta}]; \\
\tau_{\psi,d} &= K_\psi \dot{\psi}_e + K_{\dot{\psi}} \dot{\psi}_e = K_\psi (\psi_d - \psi) - K_{\dot{\psi}} \dot{\psi}.
\end{aligned}$$

The thrust and torque generated by the quadcopter's rotors are proportional to the superposition of the square of rotor speeds. However, these values are influenced by aerodynamic conditions and external disturbances. To account for these uncertainties, a parameter variation is introduced into the thrust and torque model and compensated through the added NN controller. Table II represents the parameter variation bounds, indicating the extent to which actual thrust and torque may deviate from their commanded values. Modeling these variations ensures that the model accounts for the real-world discrepancies, enhancing robustness of the control design.

TABLE II: Parameter Variation

α_1	Thrust variance	$[-0.05, 0.05]$
α_2	Roll torque variance	$[-0.05, 0.05]$
α_3	Pitch torque variance	$[-0.05, 0.05]$
α_4	Yaw torque variance	$[-0.05, 0.05]$

Therefore, the quadcopter dynamics with parameter variation and nominal controller becomes:

$$f(s, u, \alpha) = \begin{bmatrix} \dot{x} \\ \dot{y} \\ \dot{z} \\ p + S_\phi T_\theta q + C_\phi T_\theta r \\ C_\phi q - S_\theta r \\ \frac{S_\phi}{C_\theta} q + \frac{C_\phi}{C_\theta} r \\ \frac{(1+\alpha_1)T}{m} (C_\psi S_\theta C_\phi + S_\psi S_\phi) - \frac{D_x}{m} \dot{x} \\ \frac{(1+\alpha_1)T}{m} (S_\psi S_\theta C_\phi - C_\psi S_\phi) - \frac{D_y}{m} \dot{y} \\ -g + \frac{(1+\alpha_1)T}{m} (C_\theta C_\phi) - \frac{D_z}{m} \dot{z} \\ \left((I_{yy} - I_{zz})qr + (1 + \alpha_2)\tau_\phi \right) / I_{xx} \\ \left((I_{zz} - I_{xx})pr + (1 + \alpha_3)\tau_\theta \right) / I_{yy} \\ \left((I_{xx} - I_{yy})pq + (1 + \alpha_4)\tau_\psi \right) / I_{zz} \end{bmatrix}, \quad (10)$$

$$\begin{aligned}
\text{where } T &= mg - K_z z + u_1 + u_2 + u_3 + u_4; \\
\tau_\phi &= K_\phi (K_y y - \phi) + K_{\dot{\phi}} [K_y \dot{y} - \dot{\phi}] + \frac{1}{\sqrt{2}} (-u_1 - u_2 + u_3 + u_4); \\
\tau_\theta &= -K_\theta (K_x x + \theta) - K_{\dot{\theta}} (K_x \dot{x} + \dot{\theta}) + \frac{1}{\sqrt{2}} (-u_1 + u_2 + u_3 - u_4); \\
\tau_\psi &= -K_\psi \psi - K_{\dot{\psi}} \dot{\psi} + b(u_1 - u_2 + u_3 - u_4).
\end{aligned}$$

The system equation (10) consists of 12 states, 4 control inputs, and 4 parameter variations. The coordinates are shifted such that the equilibrium point is at the origin, i.e., $(x_d, y_d, z_d, \psi_d) = (0, 0, 0, 0)$. With this coordinate shift, so that $(x_d, y_d, z_d, \psi_d) = (0, 0, 0, 0)$, it follows that nominal Position and Attitude controllers are state-feedback. Table III lists the parameter values for the nominal controller, which is chosen to ensure that the state matrix associated with the

nominal controller, A_K , is stable with all its eigenvalues having negative real parts, i.e., the nominal controller stabilizes the linearized nominal system under zero parameter variation around the equilibrium point.

TABLE III: PD control gain

K_x, K_y	P gain of x/y-direction	0.05
K_z	P gain of z-direction	0.1
K_ϕ, K_θ	P gain of ϕ/θ rotation	0.1
K_ψ	P gain of ψ rotation	0.1
$K_{\dot{\phi}}, K_{\dot{\theta}}$	D gain of ϕ/θ rotation	0.01
$K_{\dot{\psi}}$	D gain of ψ rotation	0.1

B. Maximal Lipschitz Bound and Safety Domain

The feasibility of the LMI constraint (8) depends on system nonlinearity, safety domain, and parametric bound, and when feasible, one can find $(L, K, P, \Lambda, \{\lambda_{ij}\})$ that satisfy the LMI constraint so that the system (5) under the control $\pi(s) = Ks + \pi_{NN}(s)$; $\pi_{NN} \in \Pi_L$ is certified as asymptotically stable with the Lyapunov function $\mathcal{V} = s^T P s$ having a RS-RoS (Robust Safe Region of Stability) that is a sublevel set of \mathcal{V} . To maximize the class of robust, safe, and stable NN controllers, L should be as large as possible, and to maximize the size of RS-RoS the corresponding safety domain \mathcal{S} should also be as large as possible. Maximal (L, \mathcal{S}) values are determined through the iterative search method of [1, Algorithm 1]. The process begins with an initial guess (L_0, \mathcal{S}_0) set to small values, which for our quadcopter case is set as below:

$$L_0 = 1.0; \mathcal{S}_0 \equiv \begin{bmatrix} \mathcal{S}_0(x) = \mathcal{S}_0(y) \\ \mathcal{S}_0(z) \\ \mathcal{S}_0(\phi) = \mathcal{S}_0(\theta) = \mathcal{S}_0(\psi) \\ \mathcal{S}_0(\dot{x}) = \mathcal{S}_0(\dot{y}) \\ \mathcal{S}_0(\dot{z}) \\ \mathcal{S}_0(p) = \mathcal{S}_0(q) = \mathcal{S}_0(r) \end{bmatrix} = \begin{bmatrix} (-1.5, 1.5) \\ (-0.3, 0.3) \\ (-0.2, 0.2) \\ (-1.5, 1.5) \\ (-0.3, 0.3) \\ (-0.2, 0.2) \end{bmatrix}.$$

The (L, \mathcal{S}) values are iteratively increased, and the feasibility of the LMI constraint is evaluated at each step. If the LMI constraint becomes infeasible, (L, \mathcal{S}) is reduced, and the feasibility is rechecked. This process is repeated with progressively smaller step sizes, until the algorithm converges to the maximal Lipschitz bound and safety domain, denoted as (L^*, \mathcal{S}^*) , which in our case is found to be:

$$L^* = 1.330; \mathcal{S}^* \equiv \begin{bmatrix} \mathcal{S}^*(x) = \mathcal{S}^*(y) \\ \mathcal{S}^*(z) \\ \mathcal{S}^*(\phi) = \mathcal{S}^*(\theta) = \mathcal{S}^*(\psi) \\ \mathcal{S}^*(\dot{x}) = \mathcal{S}^*(\dot{y}) \\ \mathcal{S}^*(\dot{z}) \\ \mathcal{S}^*(p) = \mathcal{S}^*(q) = \mathcal{S}^*(r) \end{bmatrix} = \begin{bmatrix} (-1.9951, 1.9951) \\ (-0.3990, 0.3990) \\ (-0.2660, 0.2660) \\ (-1.9951, 1.9951) \\ (-0.3990, 0.3990) \\ (-0.2660, 0.2660) \end{bmatrix}.$$

C. Optimal NN Controller Training

To optimally train the NN controller satisfying the maximal Lipschitz bound L^* found above to minimize control cost and reference tracking error, we employ Proximity Policy Optimization (PPO) [15], a deep reinforcement learning (RL)

method based on an actor-critic structure. In an RL, an agent interacts with the environment to collect samples, where each sample is represented as (s, a, r, γ, s') where $s \in \mathcal{S}, a \in \mathcal{A}$ are the current state and action (\mathcal{S} and \mathcal{A} are state and action domains), $r \in \mathbb{R}$ is the associated reward, $\gamma \in [0, 1)$ is a discount factor, and $s' \in \mathcal{S}$ is the next state. These samples represent the transition from s to s' when the action a taken, and the reward r is received. Using the collected samples, policy and value networks are trained, where neural networks are used as function approximators, representing maps from state to action (actor network) and from state to value (value network), value is the accumulated total rewards (long-term expected return). (In contrast, the reward is an immediate return of a single step.) The goal of RL is to optimize the policy parameters to maximize value, thereby improving the agent's performance in achieving its objectives.

Fig 3 illustrates this actor-critic framework used in the optimal NN training process. The environment models the quadcopter dynamics along with the nominal controller described in Equation (10). The NN controller provides control inputs that are fed into the environment, while the environment returns a reward value for each action depending on the current state, and also advances the state. The ‘‘advantage’’ is defined as the difference between the state value and an action value, providing a measure of whether a particular action is better or worse than the default action suggested by the policy. We estimated the advantage using the method proposed in [16], and computed the policy gradient based on this estimated advantage.

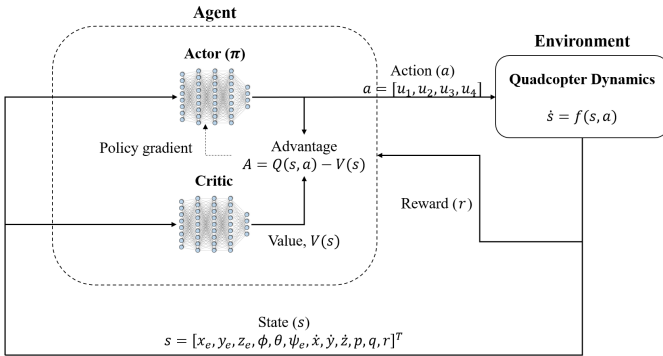


Fig. 3: Actor Critic Framework

The reward indicates how effectively the agent performs in achieving the desired objective, guiding the optimization of the policy. We design a reward function to minimize the error between the reference state and the current state. When controlling the quadcopter, two aspects of performance are considered: 1) transient response and 2) steady-state response. When the quadcopter is far from the reference position, its reward is computed from only the positional and directional errors. Once the quadcopter is close to the reference position, angular velocity, that must become small, is also penalized (along with the positional and directional errors) to reduce the oscillations around the reference. Given the position and direction errors defined as $p_e := [x_d - x, y_d - y, z_d - z]^T$ and $\psi_e := \psi_d - \psi$, and the angular velocity defined by $\nu :=$

$[p, q, r]^T$, the reward function is formulated to capture these objectives:

$$r = \begin{cases} 0.8r_{pos} + 0.2r_{\psi} & p_e > 0.3 \\ 0.6r_{pos} + 0.2r_{\psi} + 0.2r_{\nu} & \text{otherwise} \end{cases}$$

where $r_{pos} = e^{-2\|p_e\|}, r_{\psi} = e^{-|\psi_e|}, r_{\nu} = e^{-2\|\nu\|}$.

Fig 4 shows the actor and critic network structures. The actor consists of five hidden layers, each containing 64 neurons with Rectified Linear Unit (ReLU) as the activation function. The final layer performs only linear operations without an activation function. The actor has two output branches: one computes the mean, and the other computes the variance of the action. Actions are sampled from a multivariate normal distribution using the mean and variance. During testing, the variance output is ignored, and deterministic actions (mean values) are used to control the quadcopter. The critic network consists of four hidden layers, each with 192 or 256 neurons and ReLU activation function. This network evaluates the value function, guiding the optimization of the actor network.

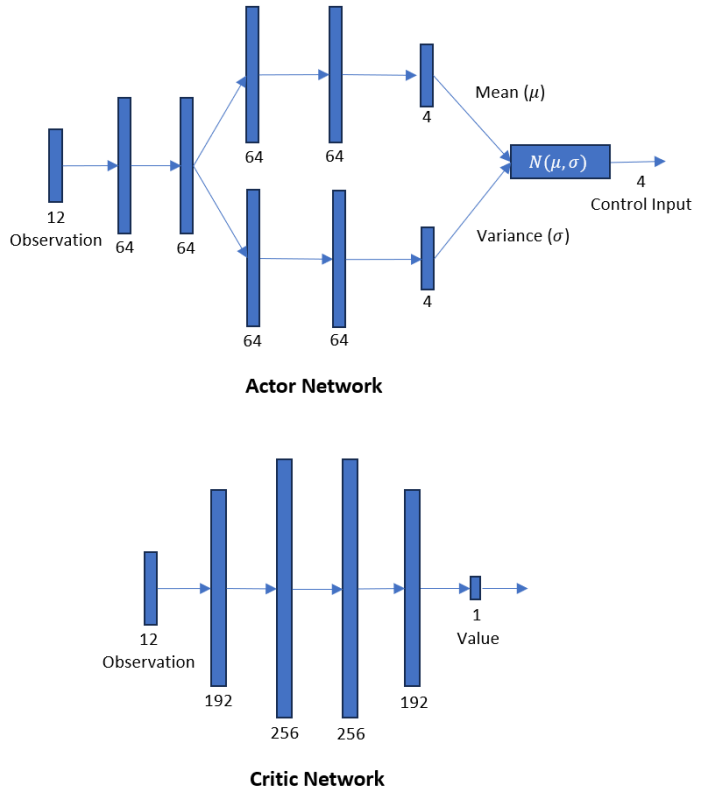


Fig. 4: Actor and Critic networks

At the beginning of each episode, the quadcopter's position is initialized at the origin, and the reference position is randomly selected within two-meter radius from the origin. Parameter variation (α) is randomly sampled at every timestep from a uniform distribution within the given bounds, introducing uncertainties in thrust and torque. The simulation uses the first-order integration to update the state based on (10). Both actor and critic networks are trained using PPO. Table

V provides the PPO parameters used for training. Definitions of these parameters can be found in [15], [16], and [17].

TABLE IV: PPO parameter

Clip Factor	0.2	Actor learning rate	0.001
Discount Factor	0.99	Critic learning rate	0.01
GAE Factor	0.95	Experience horizon	2048
Entropy loss weight	0.4	Minibatch size	2048

To certify the asymptotic stability of the closed-loop system, the Lipschitz constant of the NN controller must remain below the maximal Lipschitz bound L^* computed in Section IV-B. It is therefore important to obtain a tight estimation of an NN’s Lipschitz constant. To achieve this, we apply the semi-definite programming based estimation method proposed in [5] to estimate the Lipschitz constant of the trained actor network (without the variance branch). When the estimated Lipschitz bound of the trained NN is higher than the L^* value, we scale down the weights of the final layer of the actor network so that the maximal Lipschitz bound is satisfied. In our study, the Lipschitz constant of the trained actor network came out to be $L = 3.1519 > L^* = 1.3301$. So we scaled down the weight of the final layer by a factor smaller than $0.4 < L^*/L = 0.4220$. After adjusting the weights of the NN controller, its Lipschitz constant is reduced to below the bound:

$$L^{new} = 1.2608.$$

Note since in our design, the final layer is a linear operation without an activation function, scaling it down does not alter the action pattern inferred by the actor network. Instead, it simply reduces the magnitude of the outputs, ensuring that the Lipschitz constant remains below the required bound. This adjustment ensures the controller’s stability while preserving its functional behavior.

V. CONTROLLER EVALUATION

We evaluate the performance of the quadcopter under the nominal and NN controllers in simulation. To show the robustness of control, the parameter α is randomly drawn from the uniform distribution within the specified parameter bound.

A. Reference Position Tracking

The reference position tracking capability of the quadcopter was evaluated under two scenarios: (1) using only the nominal controller, and (2) using both the nominal and NN controllers. The quadcopter was initialized at $p_{init} = [0, 0, 0]^T$ with zero initial attitude, velocity and angular velocity, while the reference position was set to $p_d = [1.4, 0, 0]^T$.

Control inputs from the nominal controller, the NN controller, and their combined outputs are shown in Figure 5. These inputs highlight the NN controller’s role in dynamically adjusting the system’s behavior to minimize position errors.

Figure 6 demonstrates the controller performance in terms of quadcopter position, velocity, and its positional error. In the nominal controller-only scenario (Figure 6(a), (c), (e)),

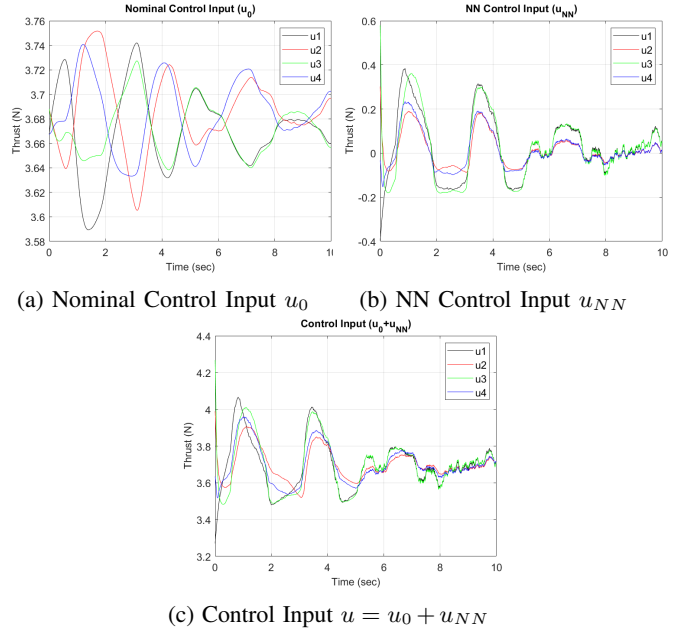


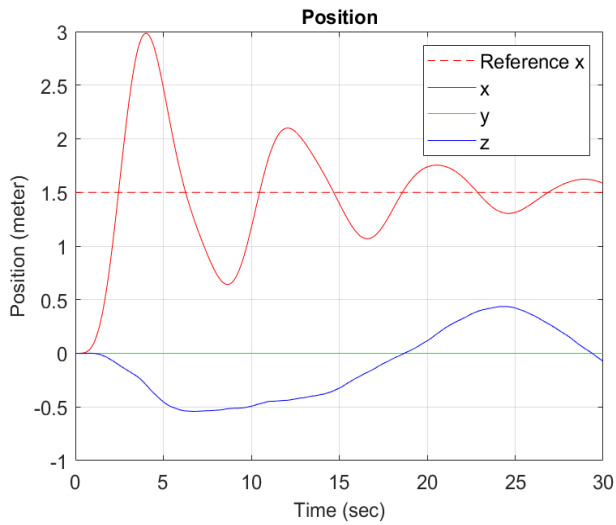
Fig. 5: Control Input

the quadcopter successfully stabilized at the reference point, but with slower error reduction. When combined with the NN controller (Figure 6(b), (d), (f)), the positional error decreased more rapidly, indicating improved transient performance. The NN controller effectively augmented the nominal controller by providing additional control inputs, leading to enhanced tracking accuracy and reduced response time, even under parameter variation.

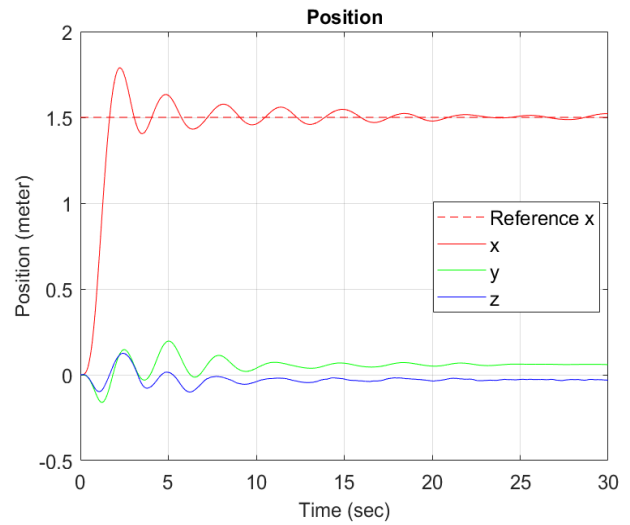
B. Reference Trajectory Tracking

To evaluate reference trajectory tracking performance, user-specified timed waypoints on an S -shaped trajectory was used as the initial specification, as listed in Table V. A path-planning algorithm of minimum snap method [18] was then used to map the timed waypoints of Table V to generate a smooth reference trajectory as a discrete time function for position, velocity, acceleration, and direction for trajectory tracking—See the red trajectory in Figure 7(a). During the control, the target position at each discrete sample time was adjusted to be the path planner’s computed position for the next sample instant, and our designed controller was employed for computing the new control action by simply changing the target position from that of the current sample instant to that of the next sample instant.

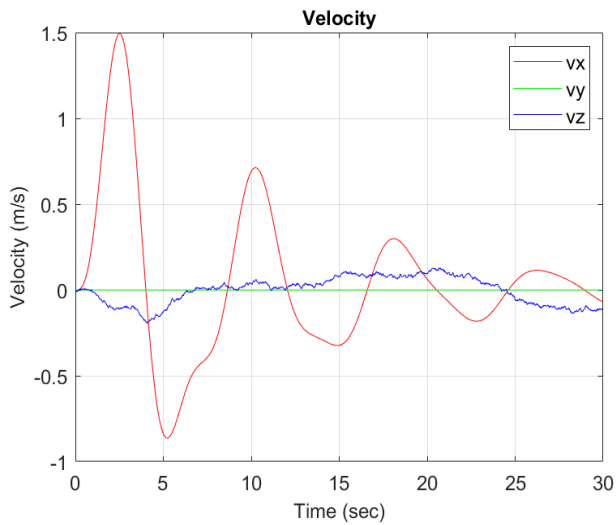
Figure 7 illustrates the quadcopter’s performance in tracking the S -shaped trajectory, where in Figure 7(a) the reference vs. actual trajectory are shown in red vs. black. The quadcopter successfully followed the reference trajectory while maintaining positional accuracy. Positional error remained low throughout the trajectory, validating the effectiveness of the NN controller in improving trajectory tracking precision even under parameter variations. The result demonstrates that the proposed control architecture is robust to environment uncertainties and capable of trajectory tracking.



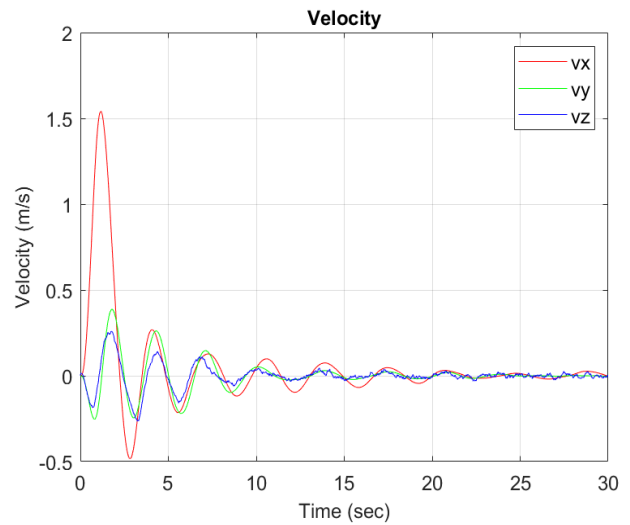
(a) Position with $\pi = \pi_0$



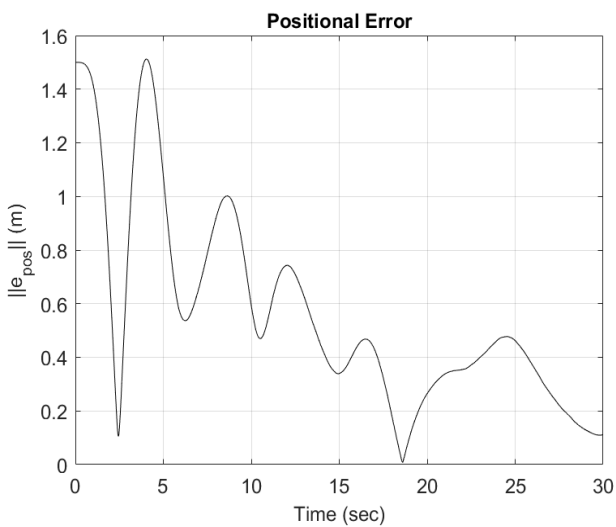
(b) Position with $\pi = \pi_0 + \pi_{NN}$



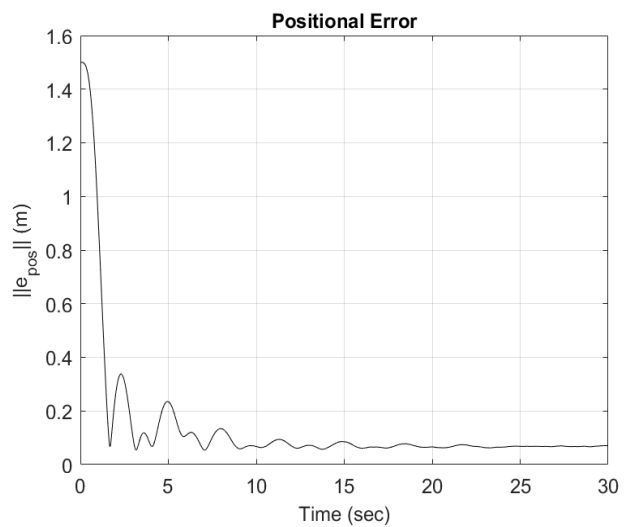
(c) Velocity with $\pi = \pi_0$



(d) Velocity with $\pi = \pi_0 + \pi_{NN}$



(e) Positional error with $\pi = \pi_0$



(f) Positional error with $\pi = \pi_0 + \pi_{NN}$

Fig. 6: Results of reference point tracking

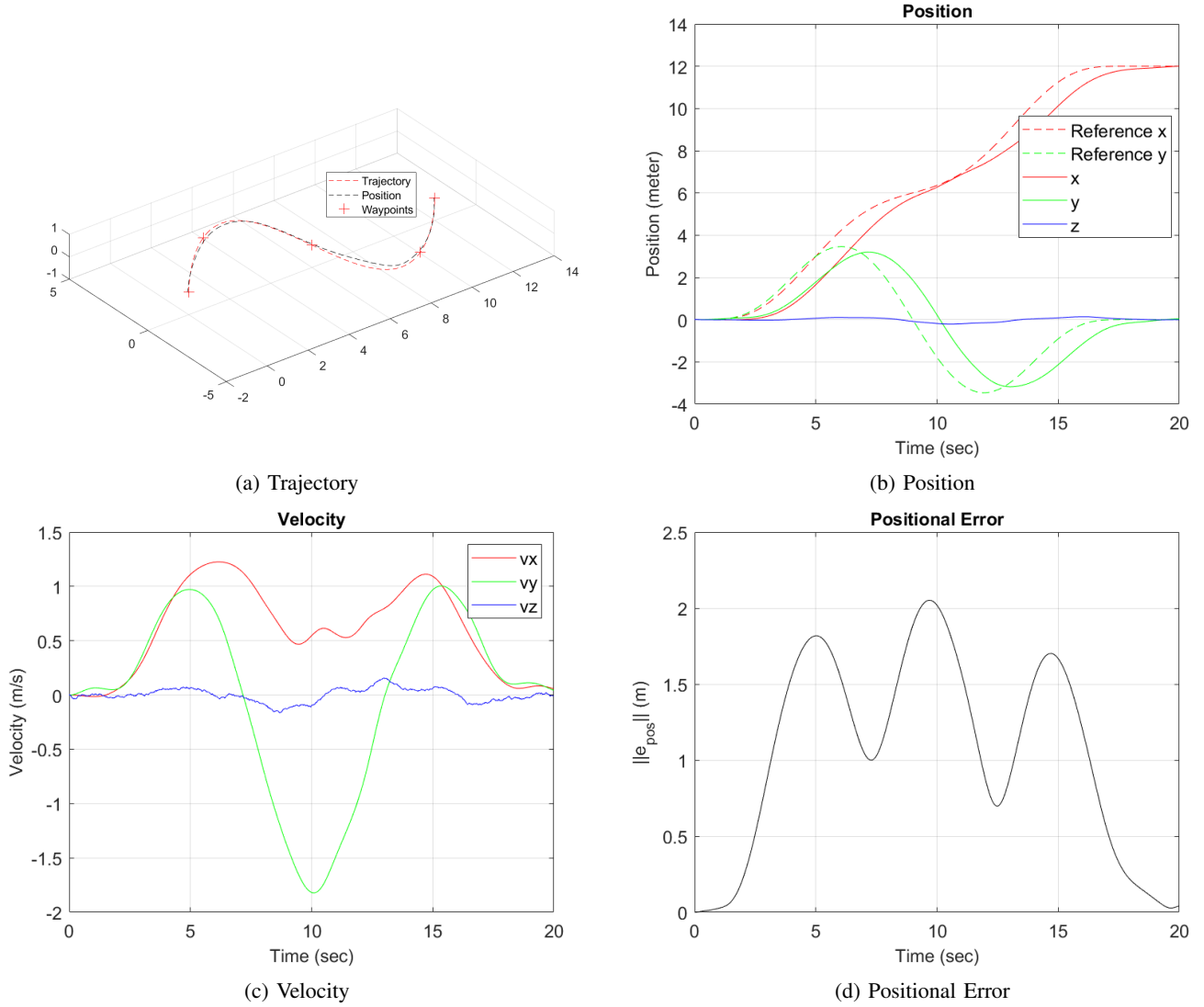


Fig. 7: Results of trajectory tracking

TABLE V: Trajectory

Waypoint	Position	Time
p_1	$[0, 0, 0]^T$	0
p_2	$[3, 3, 0]^T$	5
p_3	$[6, 0, 0]^T$	9
p_4	$[9, -3, 0]^T$	13
p_5	$[12, 0, 0]^T$	18

VI. CONCLUSION

This paper presented certain improvements in the Robust Optimal Safe and Stability Guaranteed Training (ROSS-GT) method of [1] and its successful application for control of a quadcopter for reference trajectory tracking, in the presence of thrust and torque uncertainties representing the real-world disturbances.

The evaluation showed that it is feasible to design a robust,

safe, and stability guaranteed controller for the quadcopter that also minimizes control cost and trajectory deviation, by combining the designed nominal cascaded PD controller with the designed NN controller. The addition of the NN controller further enhanced the transient/stead-state responses, demonstrating its capability to handle parameter variations effectively. The use of the robust stability-guaranteed approach ensured that the system remained asymptotically stable in spite of the parameter variations within the defined bounds.

Future work may focus on extending the method to more complex UAV models and high-fidelity simulation or real-world testing scenarios, further validating the applicability of stability-guaranteed NN controllers in practical environments.

REFERENCES

- [1] S. Talukder and R. Kumar, "Robust stability of neural network-controlled nonlinear systems with parametric variability," 2022. [Online]. Available: <https://arxiv.org/abs/2109.05710>
- [2] Y. Fan, S. Chu, W. Zhang, R. Song, and Y. Li, "Learn by observation: Imitation learning for drone patrolling from videos of a human navigator," 2020. [Online]. Available: <https://arxiv.org/abs/2008.13193>

- [3] M. Sieb, "Visual imitation learning for robot manipulation," Master's thesis, Carnegie Mellon University, Pittsburgh, PA, May, 2019.
- [4] R. S. Sutton and A. G. Barto, *Reinforcement Learning: An Introduction*, 2nd ed. The MIT Press, 2018. [Online]. Available: <http://incompleteideas.net/book/the-book-2nd.html>
- [5] M. Fazlyab, A. Robey, H. Hassani, M. Morari, and G. J. Pappas, "Efficient and accurate estimation of lipschitz constants for deep neural networks," 2023. [Online]. Available: <https://arxiv.org/abs/1906.04893>
- [6] J. Hwangbo, I. Sa, R. Siegwart, and M. Hutter, "Control of a quadrotor with reinforcement learning," *IEEE Robotics and Automation Letters*, vol. 2, DOI 10.1109/lra.2017.2720851, no. 4, Oct. 2017. [Online]. Available: <http://dx.doi.org/10.1109/LRA.2017.2720851>
- [7] W. Koch, R. Mancuso, R. West, and A. Bestavros, "Reinforcement learning for uav attitude control," *ACM Trans. Cyber-Phys. Syst.*, vol. 3, DOI 10.1145/3301273, no. 2, 2019. [Online]. Available: <https://doi.org/10.1145/3301273>
- [8] R. Polvara, M. Patacchiola, M. Hanheide, and G. Neumann, "Sim-to-real quadrotor landing via sequential deep q-networks and domain randomization," *Robotics*, vol. 9, no. 1, p. 8, 2020.
- [9] A. M. Deshpande, A. A. Minai, and M. Kumar, "Robust deep reinforcement learning for quadcopter control," 2021. [Online]. Available: <https://arxiv.org/abs/2111.03915>
- [10] M. Jin and J. Lavaei, "Control-theoretic analysis of smoothness for stability-certified reinforcement learning," in *2018 IEEE Conference on Decision and Control (CDC)*, DOI 10.1109/CDC.2018.8618996, 2018.
- [11] E. A. Paiva, J. C. Soto, J. A. Salinas, and W. Ipanaque, "Modeling and pid cascade control of a quadcopter for trajectory tracking," in *2015 CHILEAN Conference on Electrical, Electronics Engineering, Information and Communication Technologies (CHILECON)*, DOI 10.1109/Chilecon.2015.7404665, pp. 809–815, 2015.
- [12] H. Khalil, *Nonlinear Control*, ser. Always Learning. Pearson, 2014. [Online]. Available: <https://books.google.com/books?id=-WbjoAEACAAJ>
- [13] H. Gouk, E. Frank, B. Pfahringer, and M. J. Cree, "Regularisation of neural networks by enforcing lipschitz continuity," 2020. [Online]. Available: <https://arxiv.org/abs/1804.04368>
- [14] "3DR Iris - the ready to fly UAV Quadcopter — arducopter.co.uk," <https://www.arducopter.co.uk/iris-quadcopter-uav.html>, [Accessed 09-12-2024].
- [15] J. Schulman, F. Wolski, P. Dhariwal, A. Radford, and O. Klimov, "Proximal policy optimization algorithms," 2017. [Online]. Available: <https://arxiv.org/abs/1707.06347>
- [16] J. Schulman, P. Moritz, S. Levine, M. Jordan, and P. Abbeel, "High-dimensional continuous control using generalized advantage estimation," 2018. [Online]. Available: <https://arxiv.org/abs/1506.02438>
- [17] J. Schulman, S. Levine, P. Moritz, M. I. Jordan, and P. Abbeel, "Trust region policy optimization," 2017. [Online]. Available: <https://arxiv.org/abs/1502.05477>
- [18] D. Mellinger and V. Kumar, "Minimum snap trajectory generation and control for quadrotors," in *2011 IEEE International Conference on Robotics and Automation*, DOI 10.1109/ICRA.2011.5980409, pp. 2520–2525, 2011.